Chaos in a double driven dissipative nonlinear oscillator

H. H. Adamyan, S. B. Manvelyan, and G. Yu. Kryuchkyan
Yerevan State University, Manookyan 1, Yerevan, 375049, Armenia
and Institute for Physical Research, National Academy of Sciences, Ashtarak-2, 378410, Armenia
(Received 27 November 2000; published 25 September 2001)

We propose an anharmonic oscillator driven by two periodic forces of different frequencies as a time-dependent model for investigating quantum dissipative chaos. Our analysis is done in the framework of the statistical ensemble of quantum trajectories in a quantum state diffusion approach. The quantum dynamical manifestations of chaotic behavior, including the emergence of chaos, properties of strange attractors, and quantum entanglement, are studied by numerical simulation of the ensemble averaged Wigner function and von Neumann entropy.

DOI: 10.1103/PhysRevE.64.046219 PACS number(s): 05.45.Mt, 42.50.Lc, 03.65.Ta, 05.30.Ch

I. INTRODUCTION

Quantum nonlinear systems with chaotic classical counterparts have received much attention in the last two decades. This field of investigation is sometimes called ''quantum chaos'' [1]. The usual procedure for studying quantum chaos is to take a system that exhibits chaotic motion when treated classically, and see what effects occur in a quantum treatment. All real quantum systems are open and their classical limit is related to the loss of coherence produced by interaction with the environment. Thus, investigations of quantum chaotic systems are connected with the correspondence problem in general, and with decoherence and dissipation in particular.

It is now well established that the quantum dynamics of classically chaotic systems will show major departures from the classical motion on a suitable time scale. Among these phenomena we note the dynamical localization of classical diffusive excitation, due to quantum mechanical interference, which is in close analogy with Anderson localization in a random potential. Dynamical localization has been well studied theoretically [2] and verified in experiments [3] with laser-cooled atoms moving in a standing wave with periodically modulated nodal positions. Much research on the subject of classical and quantum chaos is devoted to the kicked rotor, which exhibits regions of regular and chaotic motion in the Poincaré section (see, for example, [4]). This model is very popular in investigations of the transition to quantum chaos. Its experimental realization, and observation of the model's dissipation and decoherence effects, are carried out on a gas of ultracold atoms in a magneto-optical trap subjected to a pulsed standing wave [5,6]. In Ref. [7] it was proposed to realize the parametrically kicked nonlinear oscillator model in a cavity involving Kerr nonlinearity. It was also shown that a more promising realization of this system, also including the quantum regime, is achieved in the dynamics of cooled and trapped ions, interacting with a periodic sequence of both standing wave pulses and Gaussian laser pulses [8]. Another suggestion for investigating quantum chaos in a single trapped ion was recently provided in [9]. In fact, while numerous theoretical works on the subject of quantum chaos have been carried out, their experimental realization remains somewhat scarce. Moreover, there are still many questions to be answered, and there is an obvious need for more systems showing chaos, and further experiments.

In this paper we propose a type of physical system showing dissipative chaotic dynamics. These systems are modeled by a dissipative nonlinear oscillator driven by two periodic forces of different frequencies. This model was proposed for studying quantum stochastic resonance in the authors' previous paper [10], where it was shown, in particular, that the model is available for experiments. It can be implemented at least for the dynamics of strongly interacting photons in an optical cavity with a $\chi^{(3)}$ nonlinear medium [11], and for cyclotron oscillations of a single electron in a Penning trap [12,13]. We would especially like to study the transition to quantum chaos and its control, the role of dissipation and quantum entanglement in chaotic dynamics, and related questions of characterizing quantum chaos. These investigations are complemented by consideration of the information aspect of chaotic dynamics through the von Neumann entropy.

In classical mechanics a standard characterization of chaos might be given in terms of the unpredictability of phase-space trajectories. However, the most important characteristic of classical chaotic systems—exponential divergence of trajectories, starting at arbitrarily close initial points in phase space—does not have a quantum counterpart. The question has been posed of what constitutes the quantum mechanical equivalent of chaos. Many criteria have been suggested to define chaos in quantum systems, varying in their emphasis and domain of application [14]. As yet, there is no universally accepted definition of quantum chaos. Our analysis of quantum chaos is based mainly on the time evolution of von Neumann entropy and the Wigner function.

The system under research is dissipative and therefore it has a mesoscopic nature. Quite generally, chaos in classical conservative and dissipative systems has completely different properties, e.g., strange attractors can appear only in dissipative systems. Therefore, the system of our interest might allow us to examine challenging problems of quantum dissipative chaos, including the problem of the quantum counterpart of a strange attractor. We note that, while the quantum dynamics of isolated or so called Hamiltonian systems with chaotic classical counterparts has been well studied, very

little work has been done in looking at quantum chaos of dissipative nonlinear systems. Among earlier studies of open quantum chaotic systems the papers [15] should be noted. Further impetus to increasing the dissipative quantum chaos area has recently been given by a study of decoherence and the quantum-classical correspondence problem of chaotic systems [16,17].

Below we use the traditional ensemble description of Markovian open systems, based on the master equation. This equation is presented in quantum trajectories in the framework of the quantum state diffusion (QSD) approach [18]. Recently, it was shown how quantum state diffusion can be used to model dissipative chaotic systems on individual quantum trajectories [19,20]. In contrast with these papers, here we show how it is possible to describe quantum chaos using a statistical ensemble of trajectories, which is actually realized in nature. Our results indicate that, although properties of quantum chaotic dynamics do not appear in ensemble averaged oscillatory excitation numbers, these properties are clearly seen in the entropy and Wigner function.

The outline of this paper is as follows. In the next section we describe the system proposed, and give the analysis of its classical motion on the Poincaré section in phase space. In Sec. III we develop the quantum description of the problem by numerically solving the master equation through the QSD method. We present the results for the mean excitation number of a nonlinear oscillator averaged over quantum trajectories, and for both the Wigner function and the von Neumann entropy. We summarize our results in Sec. IV.

II. MODEL OF THE DOUBLE DRIVEN OSCILLATOR: CLASSICAL PHASE MAP

In this section we give the theoretical description of the system. The nonlinear oscillator driven by two periodic forces at frequencies ω_1 and ω_2 and interacting with a reservoir is described by the following Hamiltonian:

$$H=\hbar\omega_0 a^\dagger a+\hbar\chi(a^\dagger a)^2+\hbar\{[\Omega_1\exp(-i\omega_1 t)+\Omega_2\exp(-i\omega_2 t)]a^\dagger+\text{h.c.}\}+H_{loss}, \tag{1}$$

where a and $a^\dagger$ are boson annihilation and creation operators, ω_0 is an oscillatory frequency, and χ is the strength of the anharmonicity. The couplings with two driving forces are given by Rabi frequencies Ω_1 and Ω_2. $H_{loss}=a\Gamma^\dagger+a^\dagger\Gamma$ is responsible for the linear losses of oscillatory states, due to couplings with heat reservoir operators giving rise to the damping rate γ. The reduced density operator ρ within the framework of the rotating-wave approximation, in the interaction picture corresponding to the transformation $\rho\rightarrow e^{-i\omega_1 a^\dagger a t}\rho e^{i\omega_1 a^\dagger a t}$, is governed by the master equation

$$\frac{\partial\rho}{\partial t}=-\frac{i}{\hbar}[H_0+H_{int},\rho]+\sum_{i=1,2}\left(L_i\rho L_i^\dagger-\frac{1}{2}L_i^\dagger L_i\rho-\frac{1}{2}\rho L_i^\dagger L_i\right), \tag{2}$$

where

$$H_0=\hbar\Delta a^\dagger a, \tag{3}$$

$$H_{int}=\hbar\{[\Omega_1+\Omega_2\exp[-i\delta t)]a^\dagger+[\Omega_1^*+\Omega_2^*\exp(i\delta t)]a\}+\hbar\chi(a^\dagger a)^2.$$

Here $\Delta=\omega_0-\omega_1$ is the detuning, and $\delta=\omega_2-\omega_1$ is the difference between driving frequencies, which works as a modulation frequency. L_i are the Lindblad operators

$$L_1=\sqrt{(N+1)\gamma}a, L_2=\sqrt{N\gamma}a^\dagger, \tag{4}$$

where γ is the spontaneous decay rate of the dissipation process, and N denotes the mean number of quanta of a heat bath. Note that only the case of a vacuum reservoir, $N=0$, is considered below.

For $\Omega_2=0$ this equation describes the single driven, dissipative anharmonic oscillator, which is a well-known and archetypal model in nonlinear physics [21,22]. In the semiclassical approach and in steady state this system exhibits bistability, which appears as the hysteresis behavior of the mean oscillatory number, versus either the detuning Δ or the strength of driving Ω_1 [21]. However, the hysteresis in the quantum mechanical treatment disappears in the ensemble averaged mean oscillatory number $n(t)=\langle a^\dagger(t)a(t)\rangle$, and bistability manifests itself in individual quantum trajectories, as noise-induced transitions between two possible metastable states [23], as well as in the statistics of oscillatory numbers [24].

In the case of a double driven oscillator, when two external forces are present, the corresponding Hamiltonian (3) includes explicit time dependence, even in the rotating-wave approximation. It may therefore be expected that the system presented above will exhibit regions of regular and chaotic motion depending on the parameters $\chi,\Delta,\Omega_1,\Omega_2$, and γ. To illustrate the operational regimes of the oscillator, first we pay attention to the classical description. After making the usual approximations, the classical limit of Eq. (2) becomes

$$\frac{d}{dt}\alpha(t)=-\frac{1}{2}\gamma\alpha-i[\Delta+\chi(1+2|\alpha|^2)]\alpha-i[\Omega_1+\Omega_2\exp(-i\delta t)], \tag{5}$$

where α is the dimensionless complex amplitude corresponding to the operator a. We analyze the time-dependent solution of this equation in the phase space of dimensionless position and momentum $X=\text{Re}\,\alpha$, $Y=\text{Im}\,\alpha$. There are a number of ways to make this analysis. We adopt a discrete surface or Poincaré section of this system. Let X_0, Y_0 be an arbitrary initial phase-space point of the system at the time t_0. Then we define a constant phase map in the (X,Y) plane by the sequence of points $(X_n,Y_n)=(X(t_n),Y(t_n))$, changing the time intervals by $t_n=t_0+(2\pi/\delta)n, n=0,1,2,\ldots$. This means that for any $t=t_n$ the system is at one of the points of the Poincaré section. Our analysis shows that, for extended time scales exceeding the damping rate, the asymptotic dynamics of the system is regular in the limits of small and large values of modulation frequency, i.e., $\delta\ll\gamma$ and $\delta\gg\gamma$, and also when one of the perturbation forces is much greater

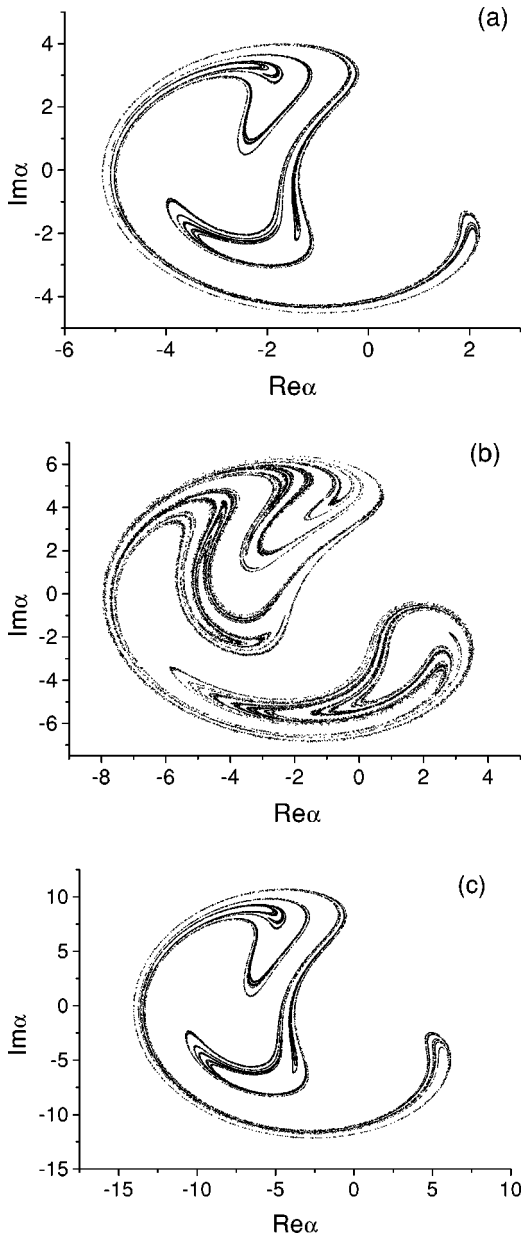

FIG. 1. Poincaré section (approximately 20 000 points) for the dimensionless classical complex amplitude of a double driven anharmonic oscillator, plotted at times of constant phase $t_n\delta=2\pi n$. The dimensionless parameters are in the region of chaos: (a) $\chi/\gamma=0.7$, $\Delta/\gamma=-15$, $\Omega_1/\gamma=\Omega_2/\gamma=10.2$, $\delta/\gamma=5$; (b) $\chi/\gamma=0.5$, $\Delta/\gamma=-25$, $\Omega_1/\gamma=\Omega_2/\gamma=25$, $\delta/\gamma=15$; (c) $\chi/\gamma=0.1$, $\Delta/\gamma=-15$, $\Omega_1/\gamma=\Omega_2/\gamma=27$, $\delta/\gamma=5$.

than the other: $\Omega_1 \ll \Omega_2$ or $\Omega_2 \ll \Omega_1$. The dynamics of the system is chaotic in the range of parameters $\delta \gtrsim \gamma$ and $\Omega_1 \simeq \Omega_2$. Figure 1 shows the results of numerical calculations of the classical maps, for parameters chosen in the range of chaos. These figures clearly indicate the classical strange attractors with fractal structure that are typical for a chaotic Poincaré section (we chose $t_0=0$ for all cases). It is expected from these results that the domain of phase space which includes an attractor strongly depends on the parameters Ω_1, Ω_2, and γ. In particular, the domain increases with increase of Ω_1 or Ω_2, and with decrease of the decay rate γ. Below we give the general consideration of this effect, considering Eq. (5) in the following integral form:

$$\alpha(t)=e^{if(t)-\gamma t/2}\left[-i\int_{t_0}^{t}(\Omega_1+\Omega_2 e^{-i\delta t_1})e^{if(t_1)}e^{\gamma t_1/2}dt_1 + \alpha(t_0)e^{\gamma t_0/2}\right]. \tag{6}$$

Here $\alpha_0=\alpha(t_0)$ is the initial value at $t=t_0$, and $f(t)$ is introduced as follows:

$$f(t)=\int_{t_0}^{t}\{\Delta+\chi[1+2|\alpha(t_1)|^2]\}dt_1. \tag{7}$$

It is easy to estimate the modulus of the complex amplitude $|\alpha(t)|$, taking into account that $f(t)$ is a real function. For its maximum value in the time interval $\alpha_{\max}=\max_t|\alpha(t)|$ we obtain

$$\alpha_{\max}\leqslant\frac{(|\Omega_1|+|\Omega_2|)}{\gamma}. \tag{8}$$

This formula determines the border of a classical map depending on the Rabi frequencies and decay rate, and explains the above conclusion about the size of the strange attractor in phase space. It is interesting that this border size for the anharmonic oscillator is independent of the parameter of nonlinearity χ and the detunings Δ and δ. This should be noted as a peculiarity of the system proposed regarding strange attractors. As can be seen from the numerical results, the attractors depicted in Fig. 1(a) and Fig. 1(c) for different parameters have the same form in phase space and differ from each other only in scale. It is obvious that this property is the consequence of a scaling symmetry of the classical equation (5). Indeed, it is easy to verify that Eq. (5) remains invariable for the scaling transformation of the complex amplitude $\alpha\rightarrow\alpha'=\lambda\alpha$, where λ is a real positive dimensionless coefficient, if the parameters χ, Δ, Ω_1, and Ω_2 are correspondingly transformed as $\chi\rightarrow\chi'=\chi/\lambda^2$, $\Delta\rightarrow\Delta'=\Delta+\chi(1-1/\lambda^2)$, and $\Omega_{1,2}\rightarrow\Omega'_{1,2}=\lambda\Omega_{1,2}$. We have illustrated such symmetry in Figs. 1(a) and 1(c) where the attractors are presented for two sets of parameters coupled by the scaling transformations. We note that in the quantum treatment the diffusion term in the master equation (2) affects the scaling symmetry roughly. In Sec. III, we will discuss this and other properties of strange attractors together with the Wigner function, in more detail.

III. QUANTUM SIGNATURES OF CHAOS: ENTROPY AND WIGNER FUNCTION

In this section we examine the problem of quantum dissipative chaos on the basis of the von Neumann entropy and the Wigner function. The peculiarities and advantages of such a consideration for interpreting quantum chaos in an ensemble theory are as follows.

The von Neumann entropy, which is defined through the reduced density operator as

$$S = -\mathrm{Tr}(\rho \ln \rho), \tag{9}$$

is a measure of dissipation and decoherence. The entropy for an isolated quantum system does not change under time evolution. If the time evolution of the system is perturbed through interaction with the environment, the averaging over the perturbation typically leads to an entropy increase. The von Neumann entropy also is a sensitive operational measure of entanglement, as well as a measure of the purity of quantum states [25]. If the system is in a pure state, the entropy is precisely zero. Thus, it is expected that study of the entropy (9) for a doubly driven oscillator will allow us to examine chaos in terms of quantum entanglement.

For an extended time-evolution period the classically chaotic system at moments $t_n = t_0 + (2\pi/\delta)n$, $n = 0,1,2,\ldots$, fills the Poincaré section in phase space. There are a number of methods to treat the Poincaré section quantum mechanically. We note Ref. [26], where a method of quantization of classical dissipative maps was proposed. The Poincaré section of one quantum trajectory was considered in [19,20]. For our dynamical model we adopt the method of the Wigner function and study the correspondence between the Wigner function, which is taken at one of the moments $t = t_n = t_0 + (2\pi/\delta)n$, and the Poincaré section. The correspondence was obtained through a computer simulation of the Wigner function.

We analyze the problem of dissipation on the basis of the QSD method, which operates with stochastic states $|\Psi_\xi(t)\rangle$, describing the evolution along a quantum trajectory. The equation of motion is

$$|d\Psi_\xi\rangle = -\frac{i}{\hbar}(H_0 + H_{int})|\Psi_\xi\rangle dt - \frac{1}{2}\sum_i (L_i^\dagger L_i - 2\langle L_i^\dagger\rangle L_i + \langle L_i\rangle\langle L_i^\dagger\rangle)|\Psi_\xi\rangle dt + \sum_i (L_i - \langle L_i\rangle)|\Psi_\xi\rangle d\xi_i . \tag{10}$$

Here ξ indicates the dependence on the stochastic process, the complex Wiener variables $d\xi_i$ satisfy the fundamental correlation properties

$$M(d\xi_i) = 0, M(d\xi_i d\xi_j) = 0, M(d\xi_i d\xi_j^*) = \delta_{ij} dt, \tag{11}$$

and the expectation value is $\langle L_i\rangle = \langle\Psi_\xi|L_i|\Psi_\xi\rangle$. According to this method the reduced density operator is calculated as the ensemble mean

$$\rho(t) = M(|\Psi_\xi\rangle\langle\Psi_\xi|) = \lim_{m\to\infty}\frac{1}{m}\sum_\xi^m |\Psi_\xi(t)\rangle\langle\Psi_\xi(t)| \tag{12}$$

over the stochastic pure states $|\Psi_\xi(t)\rangle$ describing the evolution along a quantum trajectory.

Let us first qualitatively describe the most important physical processes, which are responsible for the origin of chaotic dynamics in our QSD numerical study. There are two ways to realize the controlling transition from regular to chaotic dynamics by changing one of the parameters of the system. One of these ways is to vary the strength Ω_2 of the second force in the range from $\Omega_2 \ll \Omega_1$ to $\Omega_2 \gg \Omega_1$. In the limit $\Omega_2 \ll \Omega_1$ the system is reduced effectively to the model of a single driven anharmonic oscillator, which exhibits bistability for a definite range of parameters χ, Δ, Ω_1, and γ. In this limit our analysis of the time-dependent stochastic trajectories for expectation numbers $n_\xi(t) = \langle\Psi_\xi|a^\dagger a|\Psi_\xi\rangle$ shows that the system in the bistability range spends most of its time close to one of the semiclassical solutions of Eq. (5), with quantum interstate transitions occurring at random intervals. On increasing the amplitude Ω_2 the stimulated processes, i.e., dynamical interstate transitions, become sufficient for the other parameters chosen to lead to bistability in terms of the semiclassical solution. Their contribution at $\Omega_2 \simeq \Omega_1$ leads to the emergence of a chaotic regime in the quantum trajectories. In the limit $\Omega_2 \gg \Omega_1$ the regular dynamics is restored. This limit is equivalent to the case of $\Omega_1 \gg \Omega_2$, because we can choose an interaction picture such that the time-dependent exponent in Eq. (3) will appear near Ω_1. In fact, using the transformation $\rho \to e^{-i\omega_2 a^\dagger a t}\rho e^{i\omega_2 a^\dagger a t}$ of the reduced density operator, we arrive at the master equation (2) with the Hamiltonian

$$H_0' = \hbar(\Delta - \delta)a^\dagger a,$$

$$H_{int}' = \hbar\{[\Omega_2 + \Omega_1 \exp(i\delta t)]a^\dagger + (\Omega_2^* + \Omega_1^* \exp(-i\delta t)]a\} + \hbar\chi(a^\dagger a)^2. \tag{13}$$

This is obtained from Eq. (3) by the replacements $\omega_{1(2)} \to \omega_{2(1)}$, $\Omega_{1(2)} \to \Omega_{2(1)}$, $\Delta \to \Delta - \delta$. Nevertheless, these marginal cases differ in detail, as explained below.

In another scenario of transition to chaos the modulation frequency δ is varied, with the other parameters unchanged. In the range of small frequencies $\delta \ll \gamma$ the modulation of the system is adiabatic. So, in the range of bistability the system oscillates between the two possible metastable states. With increasing frequency, at $\delta \gtrsim \gamma$, a strong entanglement of these states occurs, and the system comes to chaos. It should be noted that, as we will show below, the transition from regular to chaotic dynamics in the classical system is marked in the quantum system by an increase of the von Neumann entropy, as well as by a strong transformation of the Wigner functions. For the case $\delta \gg \gamma$, the dynamics of the system becomes regular again.

We give the results of QSD analysis in the regimes of strong anharmonicity, considering the parameters from $\chi/\gamma = 0.7$ to $\chi/\gamma = 0.1$. The former case is strongly quantum mechanical, since the maximum mean number of oscillatory excitations is about 10, while the case $\chi/\gamma = 0.1$ corresponds to a quasiclassical regime, when the maximum oscillatory number in time is about 130. The truncated basis of Fock number states of the harmonic oscillator is used for the expansion of state vectors $|\Psi_\xi(t)\rangle$, and an initial vacuum state is chosen.

A. Time evolution of the mean oscillatory numbers

The mean excitation number of the double driven anharmonic oscillator versus time interval is of particular interest in this paper. Figures 2(a) and 2(b) depict the ensemble averaged mean oscillatory numbers $\overline{n}=\langle a^{\dagger}a\rangle$ for both cases of regular and chaotic dynamics which are realized in the classical limit. The parameters for Fig. 2(b) are chosen the same as for Fig. 1(c). The classical oscillatory number $\overline{n}=|\alpha|^2$ derived from Eq. (5) for the same parameters as the above chaotic regime is illustrated in Fig. 2(c). From these figures it is evident that while the classical result [Fig. 2(c)] shows the usual chaotic behavior, its quantum ensemble counterpart [Fig. 2(b)] has clear regular behavior. Thus, the chaotic behavior in the classical model transforms into periodic dynamics in the quantum treatment that involves ensemble averaging. These results indicate that quantum dissipative chaotic dynamics is not evident in the mean oscillatory number. Now we will show how quantum chaos emerges in both the Wigner function and the von Neumann entropy.

B. Chaos in Wigner functions and quantum interference effect

We apply the QSD to determine Wigner functions for the quantum states of a double driven anharmonic oscillator during time evolution. For this we use the well-known expression for the Wigner function in terms of the matrix elements $\rho_{nm}=\langle n|\rho|m\rangle$ of the density operator in the Fock state representation

$$W(r,\theta)=\sum_{m,n}\rho_{nm}W_{mn}(r,\theta), \tag{14}$$

where (r,θ) are the polar coordinates in the complex phase-space plane $X=r\cos\theta$, $Y=r\sin\theta$, and the coefficients $W_{mn}(r,\theta)$ are the Fourier transform of the matrix elements of the Wigner characterization function [27]

$$W_{mn}(r,\theta)=\begin{cases}\dfrac{2}{\pi}(-1)^n\sqrt{\dfrac{n!}{m!}}e^{i(m-n)\theta}(2r)^{m-n}e^{-2r^2}L_n^{m-n}(4r^2), & m\geqslant n\\ \dfrac{2}{\pi}(-1)^m\sqrt{\dfrac{m!}{n!}}e^{i(m-n)\theta}(2r)^{n-m}e^{-2r^2}L_m^{n-m}(4r^2), & n\geqslant m,\end{cases} \tag{15}$$

where L_p^q are Laguerre polynomials. In our calculation we assume that the oscillator is initially prepared in a vacuum state, and regimes of strong anharmonicity $\chi/\gamma=(0.7\text{–}0.1)$ are realized.

In Fig. 3 we demonstrate the moving of our system from regular to chaotic dynamics by plotting the Wigner function for three values of Ω_2: $\Omega_2/\gamma=1$ (a), $\Omega_2/\gamma=\Omega_1/\gamma=10.2$ (b), and $\Omega_2/\gamma=20$ (c), at a fixed moment of time. The values of $\Delta/\gamma,\chi/\gamma$, and Ω_1/γ are chosen to lead to bistability in the model of a single driven oscillator ($\Omega_2=0$).

We can see that for the case of a weak second force [Fig. 3(a)] the Wigner function has two humps, corresponding to the lower and upper levels of the excitation of the anharmonic oscillator in the bistability region. The hump centered close to $X=Y=0$ describes the approximately coherent lower state, while the other hump shows that the upper state is squeezed. The effect of squeezing is displayed as squeezing of the Gaussian. This result represents the known property of the Wigner function for the single driven anharmonic oscillator [28]. The graphs in Fig. 3 are given at an arbitrary time, exceeding the damping time. As the calculations show, for the next time intervals during the period of modulation $t=2\pi/\delta$, the hump corresponding to the upper level rotates around the central peak. When we increase the strength of the second force, the classical system reaches chaotic dynamics. The Wigner function for the chaotic dynamics is depicted in Fig. 3(b). On further increasing Ω_2, the system returns to regular dynamics. The corresponding Wigner function at an arbitrary time exceeding the transient time is presented in Fig. 3(c). It contains only one hump, rotating around the center of the phase space within the period. As mentioned above, the limit $\Omega_2\gg\Omega_1$ is physically equivalent to the opposite case $\Omega_1\gg\Omega_2$, when the system at each moment of time is close to the model of a single driven nonlinear oscillator. The difference is that the Rabi frequency Ω_2 in this case [Fig. 3(c)] is taken outside the bistability range, where the system is in the upper level. So the Wigner function has approximately the same form as the Wigner function for a single driven anharmonic oscillator, in the monostable regime of operation above threshold, when the system is excited.

As we see, the Wigner function reflecting chaotic dynamics [Fig. 3(b)] has a complicated structure. Nevertheless, it is easy to observe that its contour plots in the (X,Y) plane are generally similar to the corresponding classical Poincaré section. Now we will consider this problem in more detail, comparing the results summarized in Fig. 1 with the numerical calculations of the Wigner functions for the same sets of parameters as for the classical maps.

We present our results in Fig. 4. It can be seen in Fig. 4(a) that for the deep quantum regime ($\chi/\gamma=0.7,\Delta/\gamma=-15,\delta/\gamma=5$) the contour plot of the Wigner function is smooth and concentrated approximately around the attractor [Fig. 1(a)]. Nevertheless, the different branches of the attractor are hardly resolved in Fig. 4(a). It can also be seen that in this deep quantum regime an enlargement of the Wigner function occurs, in contrast to the Poincaré section.

Taking a smaller χ/γ, the contour plot of the Wigner function approaches the classical Poincaré section. This can

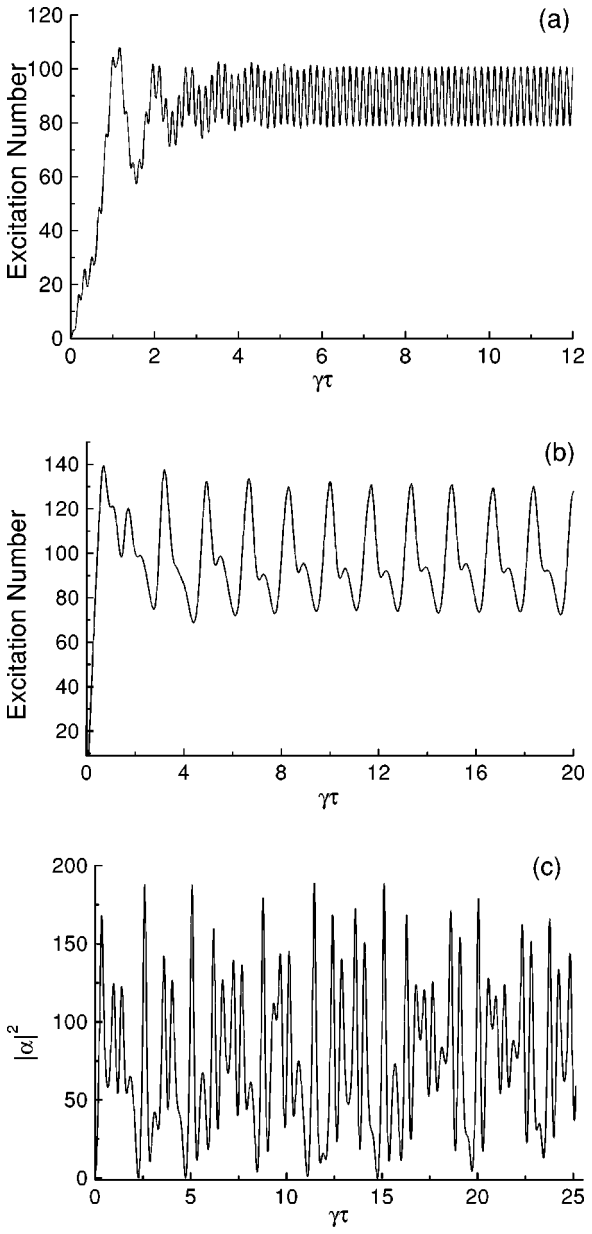

FIG. 2. (a),(b) Ensemble averaged (over 1000 trajectories) mean oscillatory numbers $\langle a^{+}a\rangle$ versus dimensionless scaled time $\gamma\tau$ for both regular (a) and chaotic (b) dynamics for parameters (a) $\chi/\gamma=0.1$, $\Delta/\gamma=-15$, $\Omega_1/\gamma=\Omega_2/\gamma=27$, $\delta/\gamma=50$; (b) $\chi/\gamma=0.1$, $\Delta/\gamma=-15$, $\Omega_1/\gamma=\Omega_2/\gamma=27$, $\delta/\gamma=5$. (c) The classical oscillatory mean number $|\alpha|^2$ for chaotic dynamics. The parameters are the same as for (b).

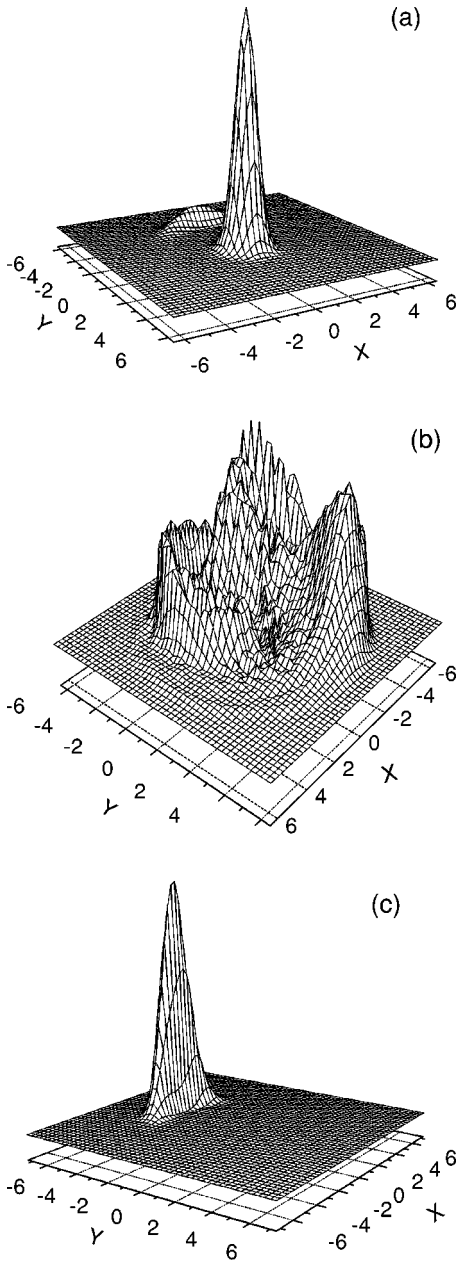

FIG. 3. Transition from regular to chaotic dynamics in the Wigner functions for three values of Ω_2/γ: $\Omega_2/\gamma=1$ (a); $\Omega_2/\gamma=10.2$ (b); $\Omega_2/\gamma=20$ (c). The parameters are $\chi/\gamma=0.7$, $\Delta/\gamma=-15$, $\Omega_1/\gamma=\Omega_2/\gamma=10.2$, $\delta/\gamma=5$. The averaging is over 2000 trajectories.

be seen in Figs. 4(b) and 4(c). For the last case the correspondence is maximal, and some details of the attractor [Fig. 1(c)] are resolved much better in Fig. 4(c). This analysis allows us also to note that the scaling symmetry of strange attractors shown in Figs. 1(a) and 1(c) disappears for the corresponding contour plots of Wigner functions [Figs. 4(a) and 4(c)] in the quantum treatment of dissipative chaos.

It should be specified that for all contour plots in Fig. 4 the corresponding Wigner functions have regions of negative values. These results are related to chaotic regimes. Obviously, this fact reflects quantum interference in the chaotic state of the system considered. It follows that the ranges of negative values of the Wigner function increase with increasing parameter χ/γ, when the system moves to the deep quantum regime. Nevertheless, ranges of negative values of the Wigner function are also observed for a comparatively small parameter χ/γ, where an operation regime close to the semiclassical is realized. This is illustrated in Fig. 5 for the parameter $\chi/\gamma=0.1$, where the mean excitation number equals 130.

Since our model is dynamical, we can also consider the correspondence between the Wigner function and the Poincaré section taken at $t_n=t_0+2\pi n/\delta$ for arbitrary t_0. Despite

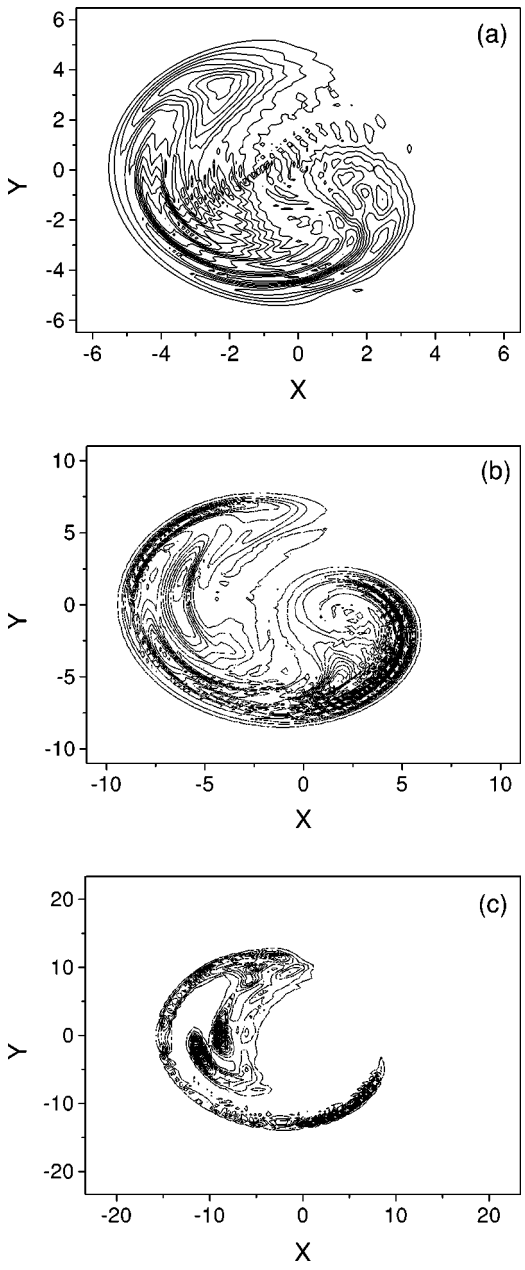

FIG. 4. Contour plots of Wigner functions corresponding to chaos. The parameters for the cases of (a), (b), and (c) are the same as in Figs. 1(a), 1(b), and 1(c), respectively. The averaging is over 2000 trajectories.

the different forms that the Wigner function and the Poincaré section have acquired, the correspondence features are the same.

C. The emergence of chaos in the von Neumann entropy

As shown in Sec. III A, quantum chaotic dynamics is not displayed clearly in the ensemble averaged oscillatory excitation number. The purpose of this subsection is merely to demonstrate how chaos is seen in the von Neumann entropy, which is one of the significant characteristics of a quantum ensemble. We also clarify other important questions in relation to quantum chaos and entanglement in the system.

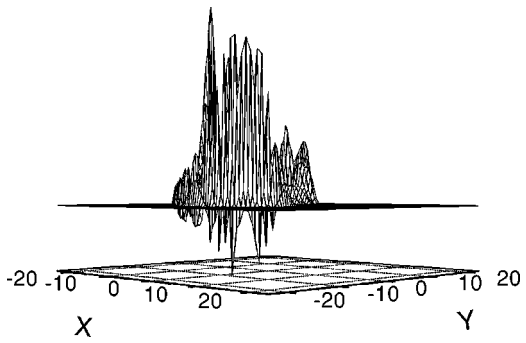

FIG. 5. Illustration of quantum interference effect on the Wigner function for the parameters $\chi/\gamma=0.1$, $\Delta/\gamma=-15$, $\Omega_1/\gamma=\Omega_2/\gamma=27$, $\delta/\gamma=5$. The averaging is over 1000 trajectories.

These analyses complete the above studies of quantum dissipative chaos in the Wigner function.

Two ways of producing chaos in a controlled manner will be considered, by monitoring the system through varying either the strength of the driving force or the difference frequency δ. We calculate the evolution of the entropy by formula (9), using the results for the reduced density matrix expressed through an ensemble of trajectories. The calculations are performed by diagonalization of the matrix ρ_{nm} in the truncated Fock state basis.

First (Fig. 6), we demonstrate the transition of the system from regular dynamics to chaos by plotting the von Neumann entropy for three values of the strength of the driving field: $\Omega_2/\gamma=1$ (a), $\Omega_2/\gamma=\Omega_1/\gamma=10.2$ (b), and $\Omega_2/\gamma=20$ (c). The same parameters are chosen as in Fig. 3 for the Wigner function. In Fig. 6(a) and Fig. 6(c) we plot the entropy evolution for regions with classically regular behavior, while Fig. 6(b) shows entropy production for chaotic motion. The essential difference between the behavior of the entropy for regular and chaotic dynamics is clearly displayed in these figures. The common feature is that, for times exceeding the time scale of transient dynamics, the entropy production in the chaotic regime dominates over the entropy production of regular dynamics. These results are in good qualitative agreement with the above results on the Wigner function, and reflect the dependence of entropy production on both the quantum entanglement and the formation of states in the system. Naturally, entropy production is stipulated by the entangling interaction between the anharmonic oscillator and its environment on the one hand, and is determined by the structure of the mixed states of the nonlinear oscillator, on the other hand. As a result, the maximal value of the entropy [Fig. 6(b)] is realized for chaotic dynamics with a large number of mixed states as depicted in Fig. 3(b), while its minimum occurs for regular dynamics with a one-hump Wigner function [Fig. 3(c)]. Also, we note that the oscillations of the entropy evident in Fig. 5 have the frequency δ. The simulations also show a definite difference between the transient times of regular and chaotic dynamics. There is some ambiguity in the definition of the transient time because of the oscillatory nature of the curves. Nevertheless, it is clearly evident that the transient time of entropy evolution for the regular case exceeds that for chaotic dynamics.

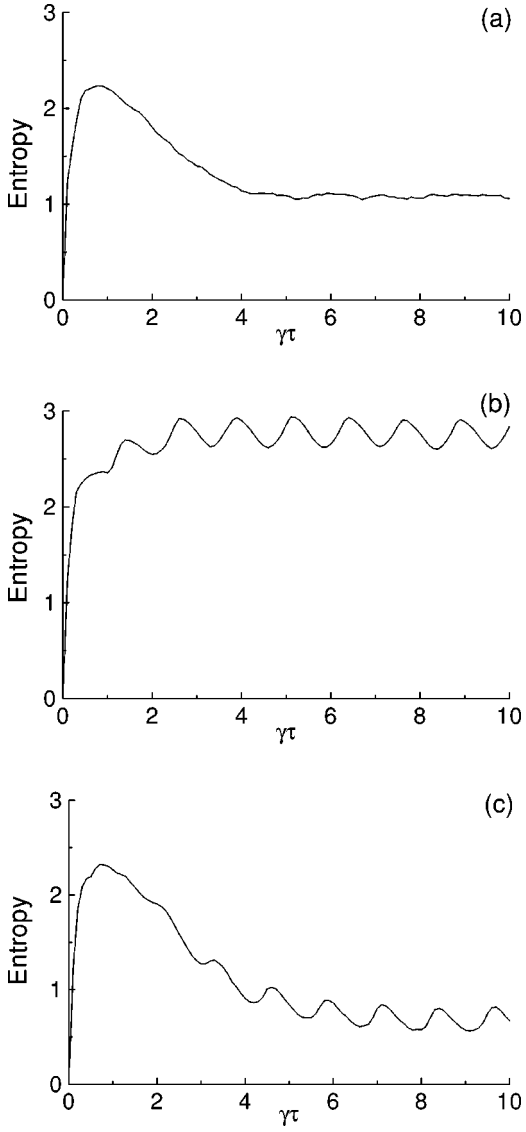

FIG. 6. Transtition to chaos in the von Neumann entropy: (a) and (c) regular dynamics, (b) chaotic dynamics. The averaging is over 2000 trajectories.

In addition to providing criteria to characterize chaos, we have also studied the behavior of the entropy versus the controlling parameters Ω_2 and δ. The results of numerical calculations at a definite time moment exceeding the transient time are presented in Fig. 7(a), where minimum values of the entropy for different Ω_2 are presented. Let us compare these results with the emergence of chaos in the classical limit. It is easy to check that for the classical case and for the parameters shown in Fig. 6 chaos appears at the critical point of $\Omega_2=\Omega_{cr}\simeq 8.195$, and disappears at $\Omega_2\simeq 12.745$. It is a well-known property of classical chaos that it appears suddenly. As is seen in Fig. 7(a), quantum chaos appears smoothly: the entropy increases as the value of Ω_2 approaches the critical value Ω_{cr}. Another way to probe chaos is to vary the detuning δ. In Fig. 7(b) the behavior of the entropy versus the modulation frequency δ is displayed.

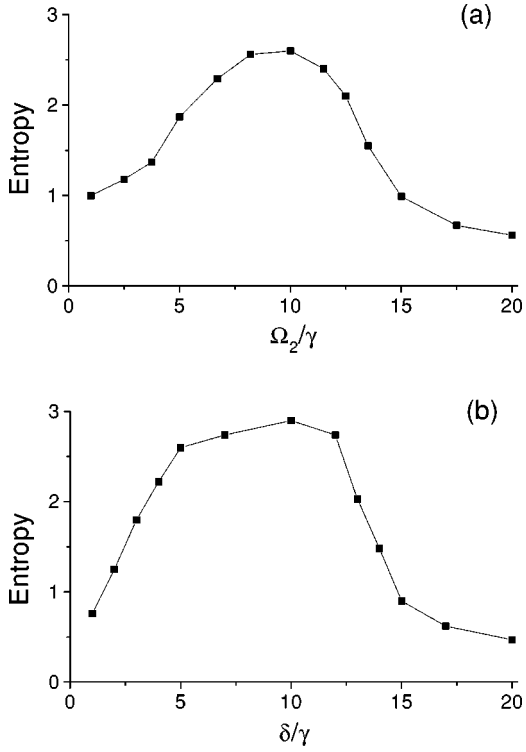

FIG. 7. Behavior of the minimal (during the period) values of von Neumann entropies versus controlling parameters. (a) Dependence of entropy on Ω_2/γ for the parameters $\chi/\gamma=0.7$, $\Delta/\gamma=-15$, $\Omega_1/\gamma=10.2$, and $\delta/\gamma=5$. (b) Dependence of entropy on δ/γ for the parameters $\chi/\gamma=0.7$, $\Delta/\gamma=-15$, and $\Omega_1/\gamma=\Omega_2/\gamma=10.2$. The averaging is over 2000 trajectories.

IV. CONCLUSION

We have presented a type of time-dependent system showing chaotic dynamics and intrinsically quantum properties. These systems are modeled by a dissipative anharmonic oscillator driven by two forces of different frequencies. We emphasize that this model is different from those using a single driven nonlinear oscillator, where a pulsed pump field could be used, and might be proposed as a possible experimental test of quantum chaos in the area of quantum optics with a continuous cw laser. The proposed model seems experimentally feasible with state-of-the-art equipment and can be realized at least in two experimental schemes. So the nonlinear behavior of a single mode field in a medium with a third order nonlinearity may provide a simple realization of the dynamics of a driven anharmonic oscillator. In fact, a single mode field is well described in terms of an anharmonic oscillator, and the nonlinear medium could be an optical fiber or a $\chi^{(3)}$ crystal, placed in a cavity. In the latter case the anharmonicity of mode dynamics comes from the self-phase modulation due to the photon-photon interaction in the $\chi^{(3)}$ medium, and dissipative effects arise from the leakage of photons through the cavity mirrors. Such a system under two driving fields is described by the Hamiltonian (1) with $a,a^{\dagger}$ being the operators of a single cavity mode. Cyclotron oscillations of a single electron in a Penning trap with a magnetic field are another realization of the quantum

anharmonic oscillator. Its anharmonicity comes from the nonlinear relativistic correction to the electron motion, while dissipative effects arise from the spontaneous emission of synchrotron radiation [12]. The trapped electron driven by a single coherent field has been experimentally realized and studied in Refs. [13]. The model we present here corresponds to the one-electron cyclotron oscillator in two coherent fields at different frequencies. The corresponding Hamiltonian is given by Eq. (1), where the operators $a,a^{\dagger}$ describe the cyclotron quantized motion at the cyclotron frequency. The values of the parameter χ/γ used in our calculations have been achieved experimentally for both the above mentioned physical systems.

The dynamics of the double driven anharmonic oscillator exhibits a rich phase-space structure, including regimes of regular and chaotic motion, with the two Rabi frequencies Ω_1 and Ω_2 and the difference δ between the driving frequencies being the control parameters. We suppose that an adequate way of investigating quantum chaos is not only the investigation of the behavior of an individual realization of trajectories, as suggested by several authors, but also a study of the dynamics of the statistical ensemble of quantum trajectories, which is naturally realized in experiments. For realization of this program of studies the quantum state diffusion simulation method based on a master equation of Lindblad form is used. We also conclude that the distinction between regular and chaotic dynamics can be most easily understood by studying the dynamics of essentially quantum properties; the von Neumann entropy and the Wigner function are only two examples. In fact, our numerical analysis has shown that the quantum dynamical manifestation of chaotic behavior does not appear in ensemble averaged oscillatory excitation numbers, but is clearly seen in the entropy and probability distributions. The connection between quantum and classical treatments of chaos was realized by means of a comparison between strange attractors on the classical Poincaré section and the contour plots of the Wigner functions. We have demonstrated that for small values of the ratio χ/γ the contour plots of Wigner functions are relatively close to the strange attractors. Indeed, as we have shown in Fig. 1(c) and Fig. 4(c), some details of the attractor are resolved on the contour plots. This similarity of quantum and classical distributions vanishes in the deep quantum regime [see Fig. 1(a) and Fig. 4(b) for $\chi/\gamma=0.7$]. An important point to emphasize is that the scaling symmetry of strange attractors in the model studied here is violated in the quantum treatment of chaos. The drastic difference between the time-dependent behavior of the von Neumann entropy for the regular and chaotic regimes is clearly displayed in Fig. 6. The von Neumann entropy indicates the connection between chaos and entanglement, and has also been used to study characteristic time scales of the emergence of chaos. For short time intervals $t<0.4\gamma^{-1}$ the entropy is a linearly increasing function of time for both the regular and chaotic regimes. For times exceeding the time scale of transient dynamics this behavior transforms to the periodic one; however, the entropy for the chaotic regime dominates over the entropy for the regular dynamics. It has also been shown that the transient time for the chaotic regime is smaller than in the regular regime.

In our analysis we have not investigated all possible quantum effects of chaotic dynamics. In particular, we have specified that the Wigner function for the chaotic regime has regions of negative values even for relatively high values of χ/γ ($\chi/\gamma=0.1$ in Fig. 5, where the mean oscillatory number $n=130$). This fact reflects the quantum interference effect in chaotic dissipative dynamics. However, we have not analyzed the correlation between the emergence of chaos and quantum interference, which is an interesting albeit complicated option for the future.

ACKNOWLEDGMENTS

This work was partially supported by INTAS Grant No. 97-1672, and by Grant No. 00375 awarded by the Armenian Science Foundation.

[1] M.C. Gutzwiller, *Chaos in Classical and Quantum Systems* (Springer-Verlag, Berlin, 1990); *Quantum Chaos, Quantum Measurement*, edited by P. Citanovic, I. Percival, and A. Wizba (Kluwer, Dordrecht, 1992); K. Nakamura, *Quantum Chaos, A New Paradigm of Nonlinear Dynamics*, Vol. 3 of *Cambridge Nonlinear Science Series* (Cambridge University Press Cambridge, 1993); *Quantum Chaos*, edited by G. Casati and B. Chirikov (Cambridge University Press, Cambridge, 1995); F. Haake, *Quantum Signatures of Chaos* (Springer-Verlag, Berlin, 2000).

[2] G. Casati, B. V. Chirikov, J. Ford, and F. M. Izrailev, *Lecture Notes in Physics* (Springer-Verlag, Berlin, 1979), Vol. 93, p. 334; S. Fishman, D.R. Grempel, and R.E. Prange, Phys. Rev. Lett. **49**, 509 (1982); G. Casati, J. Ford, I. Guarneri, and F. Vivaldi, Phys. Rev. A **34**, 1413 (1986). For a review see, for example, P.M. Koch and K.A.H. van Leeuwen, Phys. Rep. **255**, 289 (1995); M. ElGhafar, P. Törmä, V. Savichev, E. Mayr, A. Zeiler, and W.P. Schleich, Phys. Rev. Lett. **78**, 4181 (1997).

[3] F.L. Moore, J.C. Robinson, C. Bharucha, P.E. Williams, and M.G. Raizen, Phys. Rev. Lett. **73**, 2974 (1994); J.C. Robinson, C. Bharucha, F.L. Moore, R. Ianke, G.A. Geordakis, Q. Nice, M.G. Raizen, and Bala Sundaram, *ibid.* **74**, 3963 (1995); F.L. Moore, J.C. Robinson, C.F. Bharucha, Bala Sundaram, and M.G. Raizen, *ibid.* **75**, 4598 (1995).

[4] D.L. Shepelyansky, Physica D **28**, 103 (1987); F.M. Izrailev, Phys. Rep. **129**, 299 (1990).

[5] H. Ammann, R. Gray, I. Shvarchuck, and N. Christensen, Phys. Rev. Lett. **80**, 4111 (1998).

[6] B.G. Klappauf, W.H. Oskay, D.A. Staeck, and M.G. Raizen, Phys. Rev. Lett. **81**, 1203 (1998); **82**, 241 (1999).

[7] G.J. Milburn and C.A. Holmes, Phys. Rev. A **44**, 4704 (1991).

[8] J.K. Breslin, C.A. Holmes, and G.J. Milburn, Phys. Rev. A **56**, 3022 (1997); A.J. Scott, C.A. Holmes, and G.J. Milburn, *ibid.* **61**, 013401 (2000).

[9] S.A. Gardiner, J.I. Cirac, and P. Zoller, Phys. Rev. Lett. **79**, 4790 (1997).
[10] H.H. Adamyan, S.B. Manvelyan, and G.Yu. Kryuchkyan, Phys. Rev. A **63**, 022102 (2001).
[11] A. Imamoglu, H. Schmidt, G. Woods, and M. Deutsch, Phys. Rev. Lett. **79**, 1467 (1997); M.J. Werner and A. Imamoglu, Phys. Rev. A **61**, 011801(R) (2000).
[12] A.E. Kaplan, Phys. Rev. Lett. **48**, 138 (1982).
[13] G. Gabrielse, H. Dehmelt, and W. Kells, Phys. Rev. Lett. **54**, 537 (1985); D. Enzer and G. Gabrielse, *ibid.* **78**, 1211 (1997); C.H. Tseng, D. Enzer, G. Gabrielse, and F.L. Walls, Phys. Rev. A **59**, 2094 (1999).
[14] A. Peres, in *Quantum Chaos: Proceedings of the Adriatico Research Conference on Quantum Chaos*, edited by H. A. Cerdeira *et al.* (World Scientific, Singapore 1991); A. Peres, *Quantum Theory: Concepts and Methods* (Kluwer, Dordrecht, 1993); R. Schack and C.M. Caves, Phys. Rev. Lett. **71**, 525 (1993).
[15] E. Ott, M. Antonsen, Jr., and J.P. Hanson, Phys. Rev. Lett. **53**, 2187 (1984); T. Dittrich and R. Graham, Europhys. Lett. **4**, 263 (1987); Phys. Rev. A **42**, 4647 (1990).
[16] W.H. Zurek and J.P. Paz, Phys. Rev. Lett. **72**, 2508 (1994); S. Habib, K. Shizume, and W.H. Zurek, *ibid.* **80**, 4361 (1998); J.P. Paz and W.P. Zurek, e-print quant-ph/0010011.
[17] S.T. Gevorkyan, M.T. Muradyan, and G.Yu. Kryuchkyan, Phys. Rev. A **61**, 043805 (2000).
[18] N. Gisin and I.C. Percival, J. Phys. A **25**, 5677 (1992); **26**, 2233 (1993); **26**, 2245 (1993).
[19] T.P. Spiller and J.F. Ralph, Phys. Lett. A **194**, 235 (1994).
[20] T.A. Brun, I.C. Percival, and R. Schack, J. Phys. A **29**, 2077 (1996); T. Bhattacharya, S. Habib, and K. Jacobs, Phys. Rev. Lett. **85**, 4852 (2000).
[21] P.D. Drummond and D. Walls, J. Phys. A **13**, 725 (1980).
[22] D.J. Daniel and G.J. Milburn, Phys. Rev. A **39**, 4628 (1989); V. Perinova and A. Luks, *ibid.* **41**, 414 (1990); A. Bandyopadhyay and G. Gangopadhyay, J. Mod. Opt. **43**, 487 (1996); E.M. Wright, T. Wong, M.J. Collett, S.M. Tan, and D.F. Walls, Phys. Rev. A **56**, 591 (1997); D. Bortman and A. Ron, Opt. Commun. **108**, 253 (1994); Phys. Rev. A **52**, 3316 (1995).
[23] M. Rigo, G. Alber, F. Mota-Furtado, and P.F. O'Mahony, Phys. Rev. A **55**, 1665 (1997); **58**, 478 (1998).
[24] G.Yu. Kryuchkyan and K.V. Kheruntsyan, Opt. Commun. **127**, 230 (1996).
[25] S.H. Barnett and S.J.D. Phoenix, Phys. Rev. A **40**, 2404 (1989); **44**, 535 (1991); L. Gilles, B.M. Garraway, and P.L. Knight, *ibid.* **49**, 2785 (1995).
[26] R. Graham, Phys. Scr. **35**, 111 (1987).
[27] B.M. Garraway and P.L. Knight, Phys. Rev. A **49**, 1266 (1994).
[28] K.V. Kheruntsyan, J. Opt. B: Quantum Semiclassical Opt. **1**, 225 (1999).